OROBOROS O2k-Protocols

Mitochondrial Physiology Network 08.09(11):1-8 (2003-2016)
Version 10: 2016-08-11 ©2003-2016 OROBOROS
Updates: http://wiki.oroboros.at/index.php/MiPNet08.09_CellRespiration

High-resolution respirometry and coupling control protocol with intact cells: ROUTINE, LEAK, ETS, ROX

O2k-Workshop Report, IOC23, Schroecken, Austria.

Doerrier C, Gnaiger E

OROBOROS INSTRUMENTS
Schöpfstr 18, A-6020
Innsbruck, Austria
instruments@oroboros.at;
www.oroboros.at

Medical Univ of Innsbruck
D. Swarovski Research Lab
6020 Innsbruck, Austria

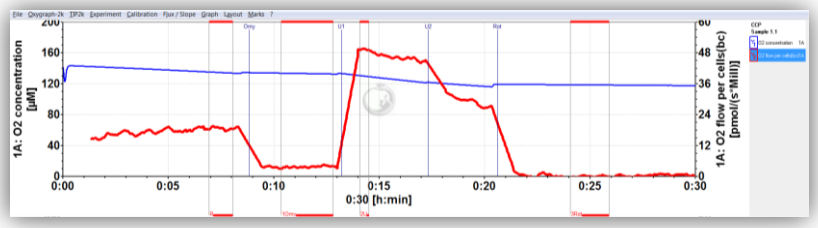

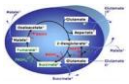

Section **Page**

Summary: High-resolution respirometry (HRR) was applied with intact cells using the coupling control protocol (CCP). A sample of leukemia cells (1 million cells/ml) was split in two 2 ml-O2k chambers operated in parallel as technical repeats. ROUTINE respiration, *R*, was 19 pmol·s^{-1}·10^{-6} cells. Oxygen concentration changed by merely 6.5 µM over a period of 5 min (<1% air saturation/min). Inhibition by oligomycin reduced respiration to 4 pmol·s^{-1}·10^{-6} in the LEAK state, *L*. Uncoupler titration stimulated electron transfer system (ETS) capacity, *E*, to 49 pmol·s^{-1}·10^{-6}. These values are corrected for rotenone-inhibited residual oxygen consumption (ROX, 1 pmol·s^{-1}·10^{-6}), in contrast to total oxygen consumption, *R'*, *L'*, and *E'* (see Figure).

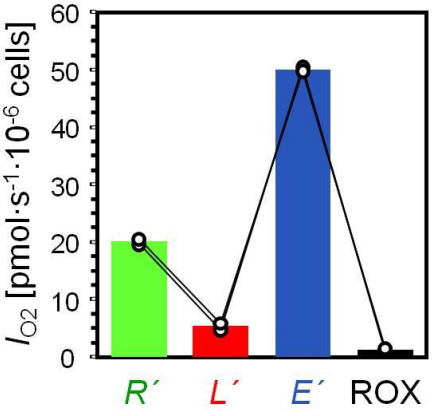

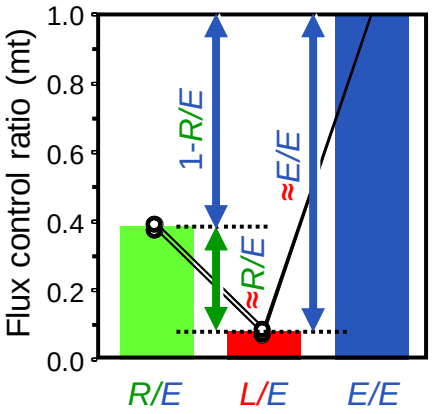

Flux control ratios, *FCR*: The ROUTINE control ratio, *R/E*, was 0.39; the LEAK control ratio, *L/E*, was 0.08. ROX was 0.02 of (uncorrected) ETS' capacity.

Flux control factors, *FCF*: The excess *E-R* capacity factor, 1-*R/E*=0.61, indicates that 61% of ETS capacity is not utilized in ROUTINE respiration. The ROUTINE coupling efficiency, ≈*R/R*=1-*L/R*=0.79 shows that 79% of *R* is 'free' ROUTINE activity, ≈*R*=*R*-*L*, used to drive phosphorylation of ADP to ATP. The ETS coupling efficiency, ≈*E/E*=1-*L/E*=0.92, was close to the upper limit of 1.0. The netROUTINE control ratio, ≈*R/E*=(*R*-*L*)/*E* was 0.30, indicating that 30% of ETS capacity was activated for ATP production.

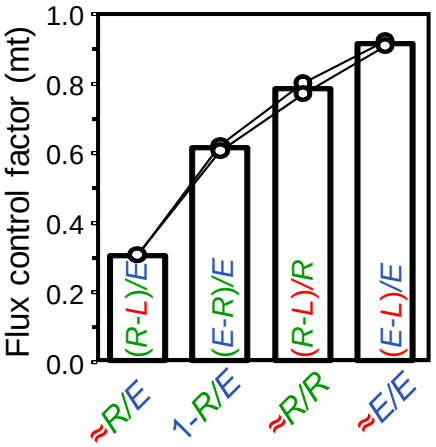

Quality control: Automatic correction for instrumental background amounted to 13% for ROUTINE respiration, but >50% and 180% for LEAK respiration and ROX, respectively, illustrating the importance of a quality-controlled correction. The experiment demonstrates the sensitivity and reproducibility of HRR with the OROBOROS Oxygraph-2k. Calibrations and routine corrections provide the basis of the high accuracy required for mitochondrial respiratory physiology and pathology. Real-time analyses combine high-resolution with instant diagnostic information. In the present update graphs illustrate several new features of DatLab 7.

1. Introduction

Small changes in cellular respiration and minor alterations in respiratory control may indicate significant mitochondrial defects, severe injuries of mitochondrial proteins or mtDNA, or decisive alterations in the state of mitochondrial signalling cascades. The standards set by the OROBOROS Oxygraph-2k for high-resolution respirometry (HRR) are required to resolve current scientific challenges in mitochondrial physiology and respiratory pathology.

HRR was refined for >20 years and the state-of-the-art instrument, the OROBOROS Oxygraph-2k (O2k) is applied world-wide, with SUIT protocols contributing significantly to the advancement of quality in the scientific literature. This communication is based on an experiment performed during an O2k-Workshop on HRR

(IOC23, Schröcken, March 2003). For the present update, files recorded with DatLab 3 were imported into the new DatLab 7 version. The experiment consisted of a single run in duplicate, using the two chambers of the O2k in parallel (Fig. 1). A control without oligomycin should be added. An O2k-Workshop experiment does not achieve a statistically complete result nor do the experimental conditions correspond to rigorous laboratory standards. The results demonstrate, however, the high reproducibility and instrumental reliability in a routine application of HRR.

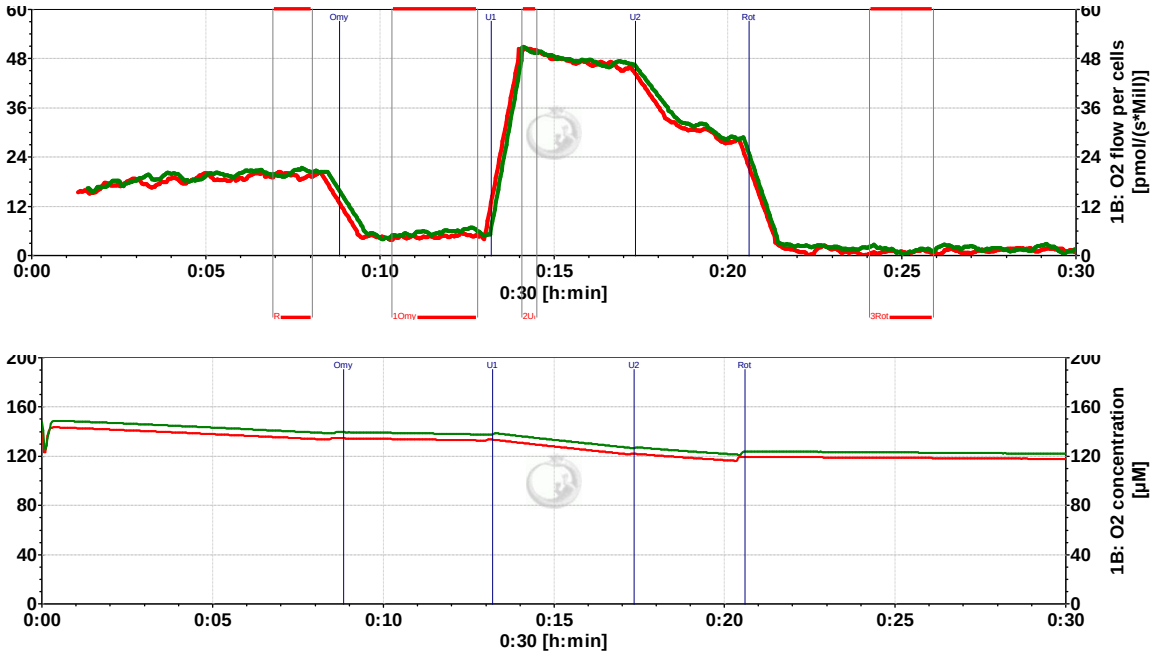

Figure 1. Superimposed traces of HRR in the two simultaneously operated O2k chambers. **A**: Cell respiration. **B**: Oxygen concentration. Y-axes scaling was edited after selecting Layout \ Reference layouts ▸ O2k-Core ▸ 05b Specific flux overlay. Experimental details: Fig. 3; DatLab file: MiPNet08.09_IntactCells.DLD.

2. Coupling control protocol

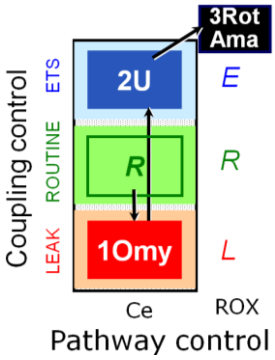

The coupling control protocol (CCP) is applied to intact cells (Fig. 1). This protocol takes 30 min, starting with a 10-min period of cellular **ROUTINE** respiration, *R*, reflecting the aerobic metabolic activity under routine culture conditions (with physiological substrates in culture medium). Three titration steps follow: **1Omy** - Oligomycin-inhibited LEAK respiration, *L*, linked mainly to compensation for the proton leak after inhibition of ATP synthase. **2U** - Uncoupler stimulated respiration, reflecting electron transfer system (ETS) capacity at noncoupled respiration, *E*. **3RotAma** – Residual oxygen consumption, ROX, after sequential inhibition of

Complex CI by rotenone and optionally CIII by antimycin A. Fluxes in states *R*, *L* and *E* are corrected for ROX. All inhibitors and the uncoupler applied in this protocol are freely permeable through the intact plasma membrane and do not require, therefore, cell membrane permeabilization (Gnaiger 2008).

Depending on quantification of cellular mass, cell volume or number, respiratory flux per volume ($J_{V,O2}$; per ml of cell suspension) is converted to an extensive quantity (flow, I_{O2}; per million cells) or a cell size-specific quantity (flux, J_{O2}; per cell protein or dry weight, cell volume). In addition to specific normalization of flux, flux control ratios (*FCR*) and flux control factors (*FCF*) are derived from the CCP protocol (Fig. 2; Gnaiger 2014).

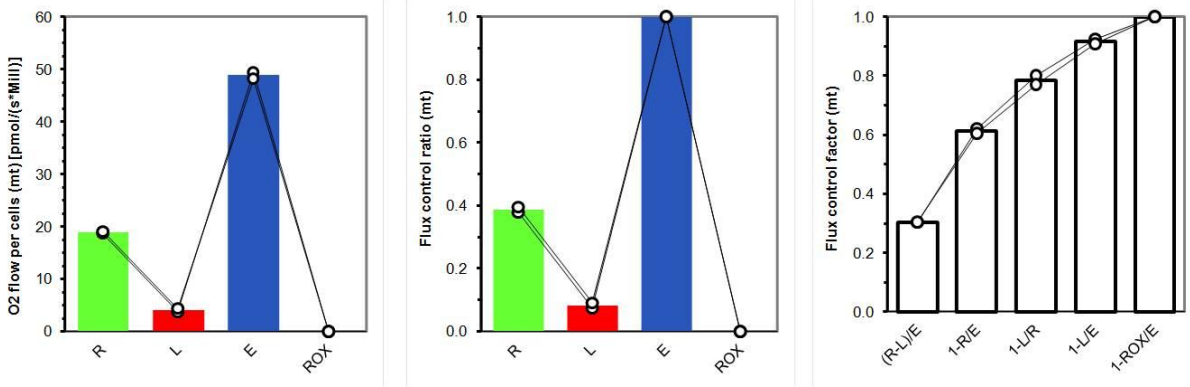

Figure 2. CCP protocol: (**A**) ROX-corrected oxygen consumption (mt) per cells. (**B**) Flux control ratios. (**C**) Flux control factors. Mark statistics F2 is copied from DatLab to the Excel template SUIT_MiPNet08.09_CellRespiration.xlsx.

2.1. ROUTINE control ratio and excess *E-R* capacity factor

R/E and $j_{ExR} = (E\text{-}R)/E = 1\text{-}R/E$

The ratio of ROUTINE respiration and ETS capacity is the *R/E flux control ratio* or ROUTINE control ratio. The corresponding *flux control factor* is the excess *E-R* capacity factor, j_{ExR}, an expression of how far ROUTINE respiration operates from ETS capacity. j_{ExR} decreases with (i) an increase of cellular ATP demand and ADP-stimulated ROUTINE respiration, (ii) partial uncoupling, and (iii) limitation of oxidative capacity by substrate supply or defects of the ETS. The inverse *R/E* ratio is the uncoupling control ratio, UCR=*E/R*.

2.2. LEAK control ratio and ETS coupling efficiency

L/E and $j_{\approx E} = \approx E/E = (E\text{-}L)/E = 1\text{-}L/E$

The ratio of LEAK respiration and ETS capacity is the *L/E* or LEAK control ratio. LEAK respiration is measured as oligomycin-inhibited respiration in intact cells.

Inhibition of ATP synthase exerts respiratory control on coupled OXPHOS, with the effect of an increased mitochondrial membrane potential and maximum proton leak or slip, which is compensated for by the LEAK respiration. The symbol ≈ expresses phosphorylation-related or net respiration, $\approx E = E - L$. In isolated mitochondria or permeabilized cells, LEAK respiration can be evaluated at defined adenylate concentrations: n, no adenylates, or T: minimum ADP concentration in the presence of ATP. Dyscoupling decreases the ETS coupling efficiency, $j_{\approx E}$. However, decreased coupling efficiency provides proof for dyscoupling only at constant ETS capacity. Alternatively, $j_{\approx E}$ may decrease in normally coupled mitochondria if ETS capacity is diminished.

2.3. NetROUTINE control ratio

$$\approx R/E = (R-L)/E$$

netR/E expresses phosphorylation-related (≈) or net respiration, $\approx R = R - L$, as a function of ETS capacity, E. It remains constant, if partial uncoupling is fully compensated by an increase of ROUTINE respiration and a constant rate of oxidative phosphorylation is maintained (Hütter et al 2004). $\approx R/E$ increases, however, upon stimulation of OXPHOS or if ETS capacity declines without effect on the rate of OXPHOS, which indicates that a higher proportion of ETS capacity is activated to drive ATP synthesis. $\approx R/E$ declines to zero in either fully uncoupled (noncoupled) cells or in cells under complete metabolic arrest. All fluxes used for calculation of the described control ratios should be corrected for non-mitochondrial respiration, estimated after inhibition of the ETS, J_{ROX}.

3. The O2k-Workshop experiment

The OROBOROS O2k was operated at 37.0 °C with 2 ml volume in both chambers. The stirring speed was at the derault of 750 rpm in both chambers, using PEEK (comparable to the new standard PVDF) stirrers. The data sampling interval was at the default of 2 s.

The main experiment on cellular respiration (Sample 1) starts after calibration of the polarographic oxygen sensors (sensor calibration), and instrumental O_2 background controls used for instrumental calibration (chamber calibration; DatLab file: MiPNet08.09_IntactCells_Calib.DLD; Supplement).

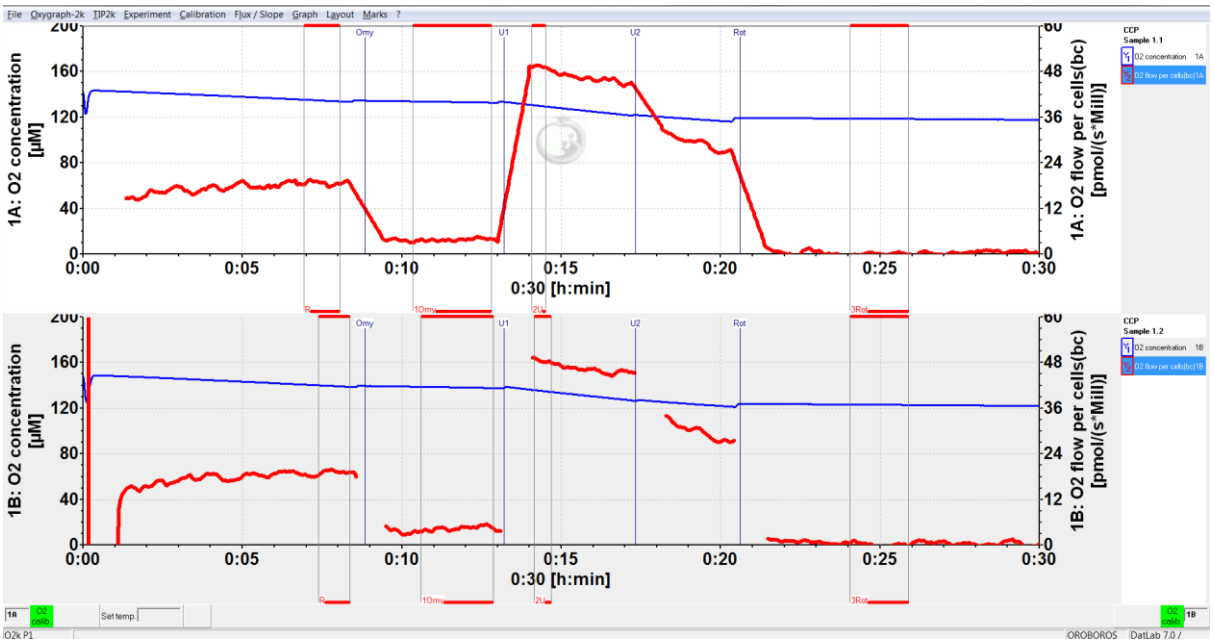

Figure 3. O2 flow per cells (bc). Screenshot from the experiment with lymphoblastoma cells suspended in RPMI selecting Layout \ Reference layouts ▸ O2k-Core ▸ 05a Specific flux and re-scaling the *Y*-axes. Parallel technical repeats in the two O2k chambers, top and bottom graph for left (A) and right chamber (B), respectively, over a 30 min period. Thin lines (blue): oxygen concentration [µM]; thick lines (red): oxygen flow per Mill cells [pmol·s^{-1}·10^{-6}] corrected for instrumental background and baseline (bc; ROX). Vertical lines are events for titrations of oligomycin (Omy: 1 µl; 2.5 µM), reducing respiration to LEAK state (inhibition of ATP synthase); FCCP (U1: 1 µM; 2 µl), stimulating respiration to the noncoupled state of the ETS; a second FCCP titration (U2: 2 µM) illustrates inhibition by excess uncoupler concentration; inhibition by rotenone (Rot: inhibitor of Complex I; 2 µl; 2.5 µM). Sections are marked for calculation of median O_2 flows F2. Calculation of flow is disturbed by titrations. Corresponding sections were marked and interpolated in chamber A (points are deleted in B). Note some salient features of high-resolution respirometry: Low respiratory activities (small changes of oxygen concentration over 20 min) yield high reproducibility in the two chambers. DatLab file: MiPNet08.09_IntactCells.DLD.

The medium used for calibration was siphoned off the glass chamber, and 2.2 ml of the lymphocyte cell suspension (1·10^6 cells/ml culture medium RPMI) was pipetted into each chamber, with the tip of the pipette held onto the wall of the glass chamber while the stirrers remained in continuous rotation. Culture media with FCS must be handled with particular care to avoid any generation of foam and inclusion of bubbles when inserting the stopper. Before closing the chamber, the cell suspension was stirred for about 2 min in contact with air for oxygenation, while subsamples may be taken for cell count and enzymatic determinations. After closing the chambers, a 5- to 10-min period is required for system stabilization, as seen in the traces of oxygen flux (Fig. 3; thick lines in red).

Table 1. (**a**) Volume-specific respiratory flux of leukemia cells [pmol $O_2 \cdot s^{-1} \cdot ml^{-1}$] after correction for instrumental background and baseline (ROX) correction. (**b**) Flux control ratios: ROUTINE control ratio, *R/E* (ratio of ROUTINE and noncoupled respiration); LEAK control ratio, *L/E* (ratio of oligomycin-inhibited and noncoupled respiration), netROUTINE control ratio, ≈*R/E*=(*R*-*L*)/*E*; and ROX/*E*' ratio (*E*' not corrected for ROX). (**c**) Flux control factors: excess *E*-*R* capacity factor, 1-*R/E*; ETS coupling efficiency, 1-*L/E*; and ROUTINE coupling efficiency, 1-*L/R*.

(**a**)

Chamber	ROUTINE	LEAK	ETS	ROX
A	18.7	3.7	49.4	0.9
B	19.1	4.4	48.2	1.4
Median	18.9	4.1	48.8	1.2

(**b**)

Chamber	***R/E***	***L/E***	***≈R/E***	***ROX/E'***
A	0.38	0.08	0.30	0.02
B	0.40	0.09	0.30	0.03
Median	0.39*	0.08#	0.30	0.02

(**c**)

Chamber	**1-*R/E***	**1-*L/E***	**1-*L/R***
A	0.61	0.92	0.80
B	0.60	0.91	0.77
Median	0.61	0.92	0.79

* UCR=*E/R* of 2.6 agrees with published uncoupling control ratios in these cells studied in mitochondrial medium (Renner et al 2003), in endothelial cells (Steinlechner-Maran et al 1996) and fibroblasts (Hütter et al 2004).

\# The corresponding respiratory control ratio, RCR=*E/L*, of 9.7 represents a state of coupling comparable to carefully isolated mitochondria.

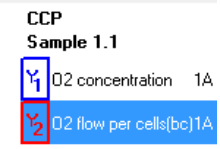

CCP titrations were performed as described above. Corresponding events indicate the titrations (Omy, U1, U2, Rot; Fig. 3).

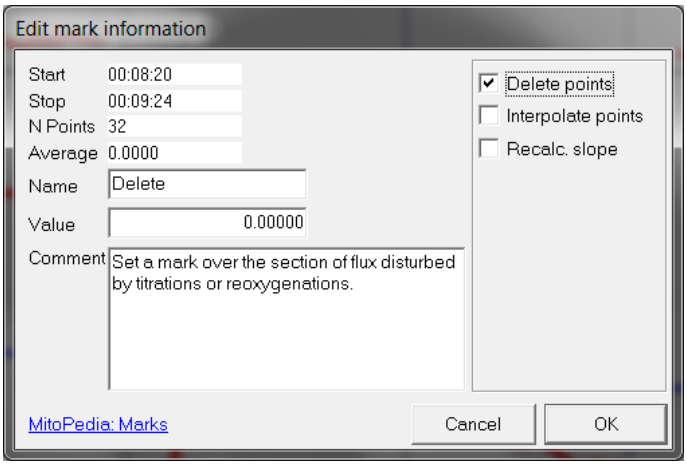

Titrations induce apparent spikes due dissolved oxygen added with each injection. After selecting a plot Y2 O2 flow per cells, set a mark across the disturbed section, and ☑ Interpolate points. Restore all points in the plot by ☑ Recalc. points.

Sections of stable flux are marked for each respiratory state. Instability of oxygen flux after the second uncoupler titration is due to progressive inhibition of cellular respiration by an excess concentration of the uncoupler illustrating the level of artifacts encountered by a single uncoupler titration. Only one mark is set at maximum ETS capacity. A prolonged period of rotenone-inhibited respiration is shown to demonstrate the instrumental stability (Fig. 3).

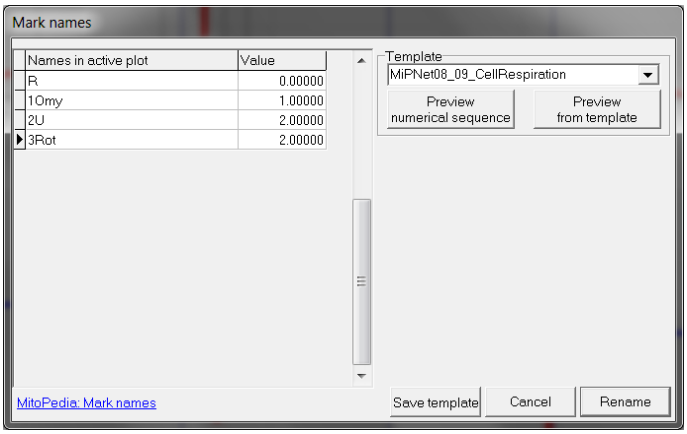

Marks are renamed using the menu Marks \ Names. Select the template ▼ MiPNet08_09_CellRespiration and click on Preview from template. Mark names are shown following the convention to add a sequential number before each abbreviated name of the titration step (1Omy, 2U, 3Rot). The values are the volumes [µl] titrated since the preceeding mark, used to calculate in the DatLab-Excel template the dilution of the sample.

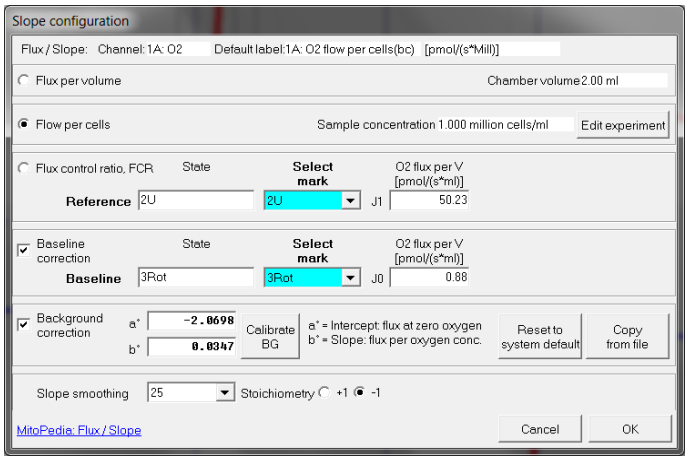

In the menu Flux/Slope, select mark ▼ 2U (*E*) as the **Reference**, and mark ▼ 3Rot (ROX) as the **Baseline**. Select ☑ Baseline correction to show the ROX-corrected plots (Fig. 3). Select ☑ Flux control ratio to obtain Fig. 4. At the data sampling interval of 2 s, ▼ Slope smoothing is set to 25 data points before setting marks.

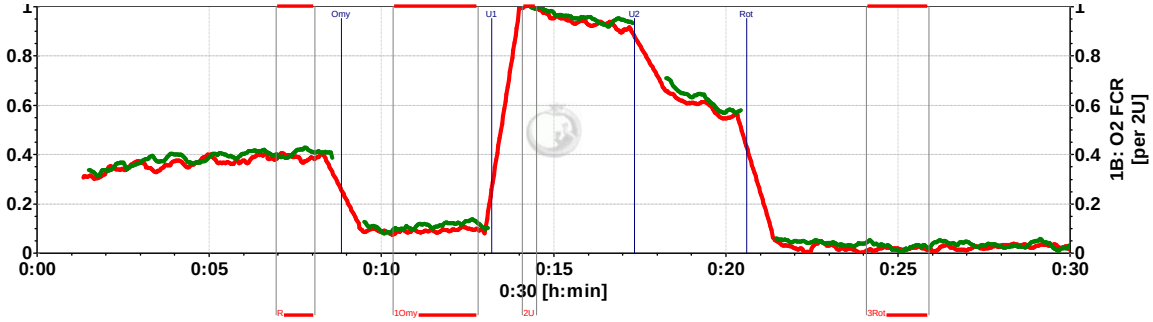

Figure 4. Flux control ratios (*FCR*), normalized to state ETS (*E*) in chambers A and B (superimposed). ROUTINE respiration in these cells is regulated at 0.40 of ETS capacity (*R'/E'*), not corrected for baseline. Oligomycin (Omy) inhibits respiration to 0.1 ETS capacity (*L'/E'*). Graph reference layout Layout \ Reference layouts ▸ O2k-Core ▸ 07b Flux control ratios overlay.

Supplementary information on the experiment, including calibration of oxygen concentration, instrumental background calibration and evaluation of respirometric measurements with emphasis on QC in high-resolution respirometry is summarized in the appended sections.

Full version and updates: *go Bioblast*
» http://wiki.oroboros.at/index.php/MiPNet08.09_CellRespiration

Supplement

A. Calibration, O_2 background correction and cell respiration

Air calibration and the O_2 background test are performed without cells.

(i) Air saturation is achieved in the aqueous solution by equilibration of the stirred medium with a gas phase.

(ii) Instrumentally-linked rates of change of oxygen concentration over time are recorded in closed chambers at various oxygen concentrations (Fig. 5).

A.1. Air calibration

O2k-SOP: MiPNet06.03 POS-Calibration-SOP

After chemical sterilization (70% ethanol for 20 min in the stirred chambers) and simultaneous temperature equilibration of the O2k (37 °C), the chambers are washed 3x with distilled water and filled with medium. The calibration signal is shown with initial default calibration parameters, and stabilizes while the stirred medium equilibrates with air in the gas phase (Fig. 5, top panel A'). A mark R1 is set over the period of a stable signal at air saturation (Fig. 5A and B; zoom in Fig. 5A').

DatLab connected to the O2k records automatically and continuously experimental temperature and actual barometric pressure. The average raw signal of the oxygen sensor [V], temperature and barometric pressure are displayed in the DatLab Calibration window after selecting Mark R1 for air calibration (Fig. 5C). The barometric pressure was 86.9 kPa or 652 mmHg (Fig. 5C) at the altitude of 1400 m in Schröcken (at a partial oxygen pressure of 16.88 kPa for moist air). The oxygen solubility factor of RPMI at 37 °C is entered as 0.89 (Fig. 5C). The oxygen concentration at air saturation, 37 °C, local barometric pressure and at 89% of the solubility of pure water, therefore, is calculated by DatLab for calibration as 158.7 µM. By comparison, air saturation at 37 °C and 100 kPa barometric pressure yields a partial oxygen pressure of 19.63 kPa for moist air, and at an oxygen solubility for pure water of 10.56 µM/kPa the standard concentration at air saturation is 207.3 µM. These calculations are performed automatically by DatLab F5.

A.2. Instrumental O_2 background

A.2.1. Oxygen signal and oxygen consumption by the POS

The raw signals of the oxygen sensors were 8.55 V and 7.71 V, as displayed for the marked calibration sections. Zero oxygen calibrations have been performed before, and the value of 0.025 V is shown in the line R0 for zero calibration. These boundary conditions resulted in calibration factors of 19.24 and 21.35 µM/V for the right and left chamber, respectively (average 20.3), at the gain setting of 4 (corresponding to a sensor current of c. 1 µA/4 V, at a gain of 4). The sensor output is, therefore, approximately (1 µA/4 V) · (1 V/20.3 µM) = 0.012 µA/µM. Based on the stoichiometry of 4 electrons per O_2 reduced at the cathode and the Faraday constant, oxygen consumption is expected at 2.591 pmol $O_2 \cdot s^{-1} \cdot \mu A^{-1}$. At air saturation (158.7 µM), this yields an oxygen consumption of the sensor of 2.592 · 0.012 · 164.1 = 5.2 pmol $O_2 \cdot s^{-1}$. In the 2 ml chamber, therefore, the expected oxygen consumption by the sensor was 2.6 pmol $O_2 \cdot s^{-1} \cdot ml^{-1}$ under the specific conditions of this experiment. This corresponds to the average instrumental background oxygen consumption measured in the O2k at air saturation, whereas the O_2 background measured during the workshop was slightly elevated (by <1 pmol $O_2 \cdot s^{-1} \cdot ml^{-1}$; Fig. 5A and B).

A.2.2. O_2 background experiment

O2k-SOP: MiPNet14.06 InstrumentalO2Background

Oxygen consumption of the polarographic oxygen sensor declines as a linear function of the oxygen signal, reaching zero at zero oxygen pressure. At low oxygen pressure, back-diffusion of oxygen into the chamber compensates for or dominates over oxygen consumption by the sensor. An instrumental background test, therefore, is required to determine the oxygen dynamics in the instrument at various oxygen levels. The instrumental O_2 background test was performed during the morning-presentation of the workshop, which explains the long duration (3.5 hours; Fig. 5) compared to a standard test completed within <2 hours.

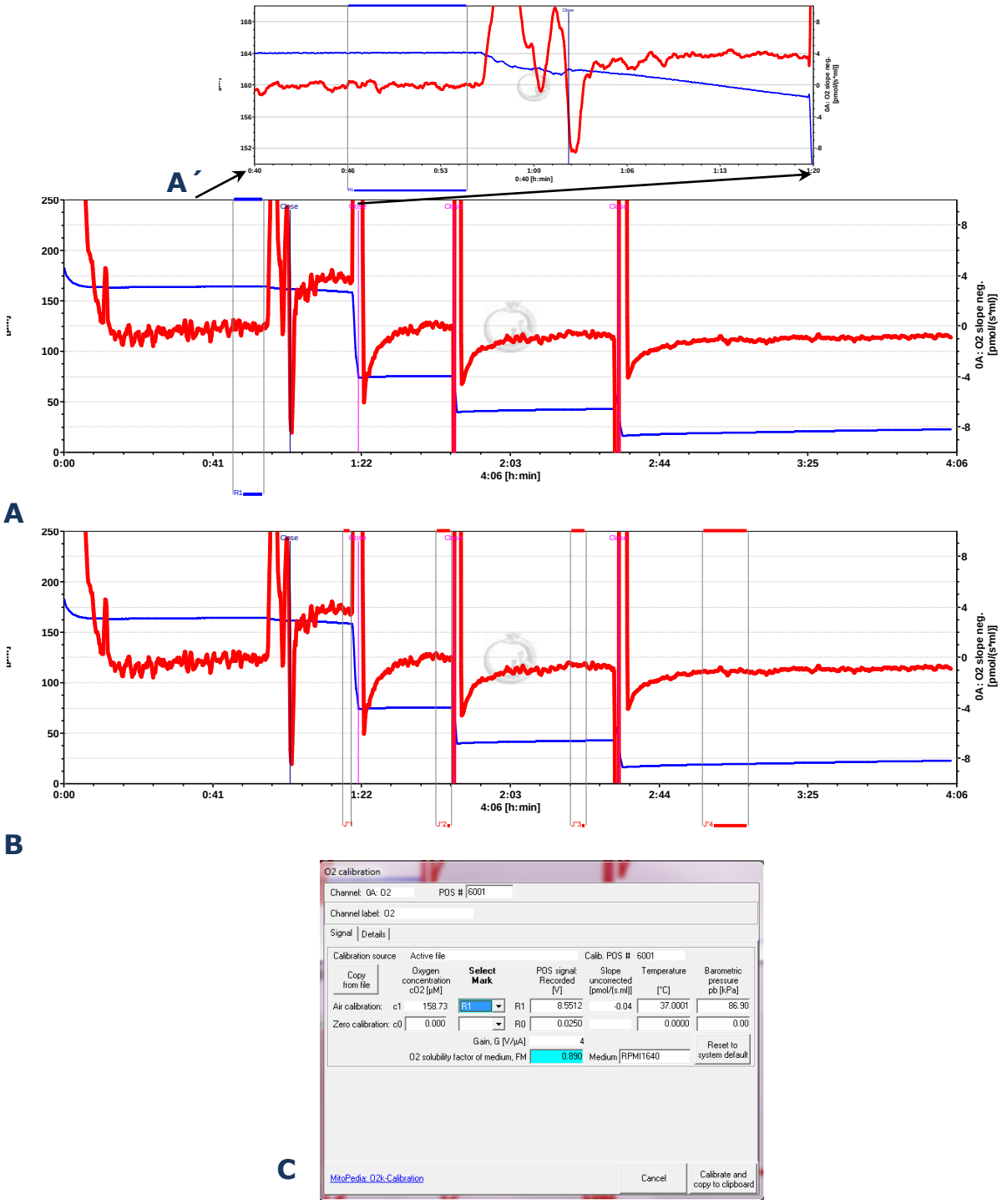

Figure 5. Air calibration and instrumental background control experiment: Overview of the calibration experiment (A and B for left and right chamber); **A'** a zoom into the calibration phase. The section of air saturation is marked (Mark R1 in **A**, yielding calibration information in panel **C**. Subsequently, instrumental O_2 background calibration is performed at four levels of oxygen concentration (marked sections shown in **B**). Experimental fluxes are shown without background correction (O2 slope neg.). DatLab file MiPNet08.09_IntactCells_Calib.DLD.

The linear dependence of background oxygen flux from oxygen concentration is described as the intercept at zero oxygen concentration (maximum back-diffusion of

oxygen) and the slope, which are typically -2 pmol $O_2 \cdot s^{-1} \cdot ml^{-1}$ for the intercept, and 0.025 for the slope. High accuracy of respiratory flux measurement requires instrumental calibration, background control experiments and corresponding corrections performed automatically by the software DatLab.

A.2.2. O_2 background and baseline correction of respiratory flux

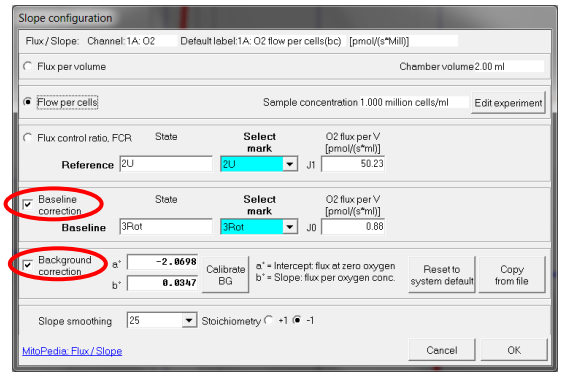

In contrast to *instrumental* O_2 ☑Background correction, the *physiological* ☑ Baseline correction can be selected to subtract ROX from the total fluxes.

The effect of instrumental background correction is small for ETS capacity (<5%), increases for ROUTINE and LEAK respiration (12% and 47%), and becomes dominating in ROX measured at high oxygen concentration (180%; Table 2 and Fig. 6). Whereas ROX was 5% of ROUTINE flux, this would be estimated at 13% with neglect of instrumental O_2 background correction.

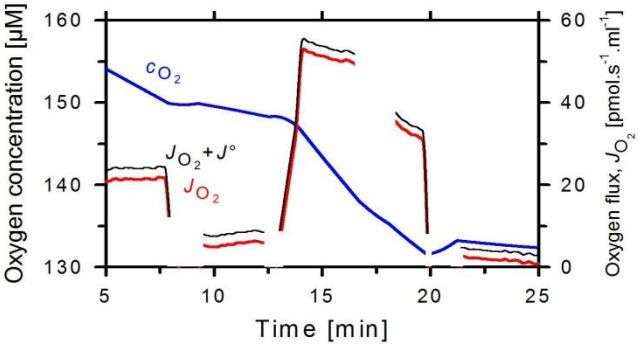

Figure 6. Cell respiration corrected for instrumental O_2 background (oxygen flux per chamber volume, J_{O2}; red line), compared to total oxygen flux including instrumental background ($J_{O2}+J°$; black thin line, uncorrected: O_2 slope neg.). At low volume-specific respiration, the decline of O_2 concentration was small (left axis, zoomed from 130 to 160 µM O_2; blue line), and the oxygen-dependent background correction is nearly constant.

High-resolution respirometry enables flux to be resolved at small changes of oxygen concentration over time (Fig. 1). When oxygen concentrations remain high, then the background correction is dominated by the oxygen consumption of the sensor. At a steeper decline of oxygen concentration, the sign of the background correction would change, when oxygen back-diffusion predominates over sensor oxygen consumption. In this case, an initial over-estimation of respiration would change to a final underestimation. In respirometers with Teflon stirrers and inappropriate sealings, the uncorrected rotenone respiration frequently appears as an increase of oxygen concentration over time.

A.3. Optimum chamber volume, resolution of flux, and instrumental background

Respiratory flux per volume increases 10-fold when using a 10-fold lower chamber volume with the same amount of biological material, thus obtaining a 10-fold higher cell density. Would reduction of the chamber volume, e.g. to 200 µl instead of 2 ml, reduce the backgroud effect? The simple answer is no, since (i) the oxygen consumption of the oxygen sensor is independent of chamber volume, whereas the volume-specific oxygen consumption increases in indirect proportion to the chamber volume. Thus the ratio of instrumental background and biological respiration remains unchanged, whereas the complications of handling microvolumes increase as chamber volume is reduced.

Table 2. Apparent volume-specific respiratory flux of leukemia cells [pmol $O_2 \cdot s^{-1} \cdot ml^{-1}$], uncorrected for non-mitochondrial respiration (compare Tab. 1), (**a**) with correction for instrumental background and (**b**) without background correction.

	Chamber	ROUTINE'	LEAK'	ETS'	ROX
(a)	A	19.6	4.6	50.3	0.9
	B	20.5	5.8	49.6	1.4
	Median	20.1	5.2	49.9	1.2
	Chamber				
(b)	A	22.2	7.2	52.7	3.0
	B	22.8	8.0	51.7	3.2
	Median	22.5	7.6	52.2	3.1

A detailed analysis of the optimum chamber volume must take into account (ii) the rapid decline of oxygen concentration, leaving little scope for any tests of respiratory stability over time and multiple titrations; and (iii) the effect of back-diffusion of oxygen. This effect of back-diffusion increases with the ratio of surface area (where diffusion takes place) to chamber volume, hence micro-chambers are more problematic in terms of oxygen leakage into the system when compared to large chamber volumes. Paradoxically, the well appreciated advantages of micro-volume chambers for high-resolution of oxygen flux when biological material is limiting, are more than offset by the increasingly dominating artefacts which remain largely ignored.

Taken together, the present experimental example illustrates the advantages of high-resolution respirometry for routine applications in cellular and mitochondrial physiology.

B. References

Gnaiger E (2008) Polarographic oxygen sensors, the oxygraph and high-resolution respirometry to assess mitochondrial function. In: Mitochondrial Dysfunction in Drug-Induced Toxicity (Dykens JA, Will Y, eds) John Wiley:327-52. »

Gnaiger E (2014) Mitochondrial Pathways and Respiratory Control. An Introduction to OXPHOS Analysis. 4th ed. Mitochondr Physiol Network 19.12. OROBOROS MiPNet Publications, Innsbruck:80 pp. »

Gnaiger E, Steinlechner-Maran R, Méndez G, Eberl T, Margreiter R (1995) Control of mitochondrial and cellular respiration by oxygen. J Bioenerg Biomembr 27:583-96. »

Hütter E, Renner K, Pfister G, Stöckl P, Jansen-Dürr P, Gnaiger E (2004) Senescence-associated changes in respiration and oxidative phosphorylation in primary human fibroblasts. Biochem J 380:919-28. »

Renner K, Amberger A, Konwalinka G, Gnaiger E (2003) Changes of mitochondrial respiration, mitochondrial content and cell size after induction of apoptosis in leukemia cells. Biochim Biophys Acta 1642:115-23. »

Steinlechner-Maran R, Eberl T, Kunc M, Margreiter R, Gnaiger E (1996) Oxygen dependence of respiration in coupled and uncoupled endothelial cells. Am J Physiol 271:C2053-61. »

» MiPNet19.18D. O_2 calibration.
» MiPNet19.18E. Oxygen flux analysis.

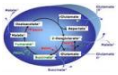

DatLab files and DatLab-Excel templates
» Files_Protocols\MiPNet08.09_CellRespiration
» MiPNet06.03 POS calibration SOP.
» MiPNet14.06 Instrumental O_2 background and accuracy of oxygen flux.

C. Author contributions

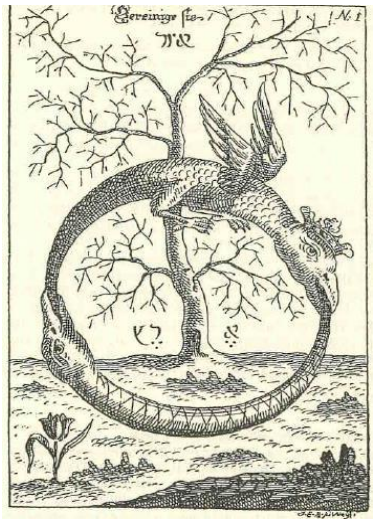

EG performed the data analysis, wrote the chapter and prepared the graphs. CD prepared the DatLab-Excel templates and co-wrote the chapter. Christina Plattner assisted in preparing the DatLab-Excel templates. Kathrin Renner performed the O2k-Workshop experiment (see previous versions).

http://www.bioblast.at/index.php/File:MiPNet08.09_CellRespiration.pdf

D. Graph layouts – specific examples

Graph layout **05a Specific flux**

For each chamber 'O2 concentration' and 'O2 flux per unit' is displayed, where unit is the unit selected in the Edit experiment window. If, e.g. mg was selected, the plot is 'O2 flux per mass'. The amount of sample (as mg, mill cells, or units) is entered in the Edit experiment window F3.

Ref: Renner K, Amberger A, Konwalinka G, Gnaiger E (2003) Changes of mitochondrial respiration, mitochondrial content and cell size after induction of apoptosis in leukemia cells. Biochim. Biophys. Acta 1642:115-23.

Info: » http://wiki.oroboros.at/index.php/O2k-Protocols

Graph layout **05b Specific flux overlay**

Graph 1: Display of O2 flux per unit (O2 flow per cells in demo file) for both chambers.

Graph 2: Display of O2-concentration for both chambers.
The fluxes of both chambers can be directly compared in one window, while both O2 concentrations are plotted in the second window.

Manual: MiPNet19.18E O2 flux analysis

O2k-Demo: High-resolution respirometry and coupling control protocol with intact cells: ROUTINE, LEAK, ETS, ROX. MiPNet08.09.

Ref: Gnaiger E (2008) Polarographic oxygen sensors, the oxygraph and high-resolution respirometry to assess mitochondrial function. In: Mitochondrial Dysfunction in Drug-Induced Toxicity (Dykens JA, Will Y, eds) John Wiley:327-52. - See Fig. 2.

Graph layout **07b Flux control ratios overlay**

Before selecting this layout, define the reference (and baseline) metabolic states in the menu Flux/Slope. Plot of flux control ratios (*FCR*) for both chambers in Graph 1. The range for the Y axes is set to 1.0. Oxygen concentration is plotted in Graph 2 for both chambers.

Manual: MiPNet19.18E O2 flux analysis

O2k-Demo: High-resolution respirometry and coupling control protocol with intact cells: ROUTINE, LEAK, ETS, ROX. MiPNet08.09
An experiment of HRR with intact cells. MiPNet10.04

Ref.: Gnaiger E (2008) Polarographic oxygen sensors, the oxygraph and high-resolution respirometry to assess mitochondrial function. In: Mitochondrial Dysfunction in Drug-Induced Toxicity (Dykens JA, Will Y, eds) John Wiley:327-52. - See Tab. 1.

Gnaiger E (2009) Capacity of oxidative phosphorylation in human skeletal muscle. New perspectives of mitochondrial physiology. Int J Biochem Cell Biol 41:1837-45.